Journal of The Electrochemical Society

The Electrochemical Society
Advancing solid state & electrochemical science & technology

OPEN ACCESS

Engineered Hierarchical CuO Nanoleaves Based Electrochemical Nonenzymatic Biosensor for Glucose Detection

To cite this article: Rafiq Ahmad *et al* 2021 *J. Electrochem. Soc.* **168** 017501

View the article online for updates and enhancements.

You may also like

- Synthesis of Self-Assembled CuO Sphere Structures and Their Glucose Sensing Characteristics
Feng-Renn Juang and Tzu-Ming Wang
- Local Homoepitaxial Growth and Optical Properties of ZnO Polar Nanoleaves
Zhang Chun-Zhi, Gao Hong, Zhang Di et al.
- Synthesis of Ag/Co_3O_4 for High Sensitive Non-Enzymatic Glucose Sensor through Synergy of Surface/Interface Engineering
Xiao Bai and Ziyin Yang

Your Lab in a Box!
The PAT-Tester-i-16: All you need for Battery Material Testing.
All-in-One Solution with integrated Temperature Chamber!
Cableless Connection for Battery Test Cells!
Fully featured Multichannel Potentiostat / Galvanostat / EIS!
www.el-cell.com +49 40 79012-734 sales@el-cell.com
EL-CELL®
electrochemical test equipment

This content was downloaded from IP address 3.142.12.170 on 17/05/2024 at 16:54

Journal of The Electrochemical Society, 2021 **168** 017501

Engineered Hierarchical CuO Nanoleaves Based Electrochemical Nonenzymatic Biosensor for Glucose Detection

Rafiq Ahmad,[1,z] Marya Khan,[1] Prabhash Mishra,[1,2] Nushrat Jahan,[1] Md. Aquib Ahsan,[1] Imran Ahmad,[1] Mohammad Rizwan Khan,[3] Yosuke Watanabe,[4] Mansoor Ali Syed,[5] Hidemitsu Furukawa,[4] and Ajit Khosla[4,*,z]

[1]*Centre for Nanoscience and Nanotechnology, Jamia Millia Islamia (Central University), New Delhi-110025, India*
[2] *Centre for Photonics and 2D Materials, Moscow Institute of Physics and Technology (MIPT), Dolgoprudny 141700, Russian Federation*
[3]*Department of Materials Science and Engineering, Incheon National University, Incheon 22012, Korea*
[4]*Department of Mechanical Systems Engineering, Faculty of Engineering, Yamagata University, Yonezawa, Yamagata 992-8510, Japan*
[5]*Department of Biotechnology, Jamia Millia Islamia (Central University), New Delhi 110025, India*

In this study, we synthesized hierarchical CuO nanoleaves in large-quantity via the hydrothermal method. We employed different techniques to characterize the morphological, structural, optical properties of the as-prepared hierarchical CuO nanoleaves sample. An electrochemical based nonenzymatic glucose biosensor was fabricated using engineered hierarchical CuO nanoleaves. The electrochemical behavior of fabricated biosensor towards glucose was analyzed with cyclic voltammetry (CV) and amperometry (i–t) techniques. Owing to the high electroactive surface area, hierarchical CuO nanoleaves based nonenzymatic biosensor electrode shows enhanced electrochemical catalytic behavior for glucose electro-oxidation in 100 mM sodium hydroxide (NaOH) electrolyte. The nonenzymatic biosensor displays a high sensitivity (1467.32 μA/(mM cm^2)), linear range (0.005–5.89 mM), and detection limit of 12 nM (S/N = 3). Moreover, biosensor displayed good selectivity, reproducibility, repeatability, and stability at room temperature over three-week storage period. Further, as-fabricated nonenzymatic glucose biosensors were employed for practical applications in human serum sample measurements. The obtained data were compared to the commercial biosensor, which demonstrates the practical usability of nonenzymatic glucose biosensors in real sample analysis.
© 2021 The Author(s). Published on behalf of The Electrochemical Society by IOP Publishing Limited. This is an open access article distributed under the terms of the Creative Commons Attribution 4.0 License (CC BY, http://creativecommons.org/licenses/by/4.0/), which permits unrestricted reuse of the work in any medium, provided the original work is properly cited. [DOI: 10.1149/1945-7111/abd515]

Manuscript received November 20, 2020. Published January 6, 2021. *This paper is part of the JES Focus Issue on Recent Advances in Chemical and Biological Sensors and Micro-Nanofabricated Sensors and Systems.*

The blood glucose concentration is the basis of diabetes mellitus "chronic and metabolic disease" diagnosis. The elevated levels of blood sugar "glucose" lead to many health problems, such as chronic kidney failure, stroke, cardiovascular disease, eyes retina damage, and foot ulcers.[1,2] Hence, early diagnosis is crucial to prevent and avoid life-threatening complications caused at abnormal glucose levels. In recent, different methods (such as electrochemical, colorimetric, piezoelectric, and thermoelectric based biosensors) have been utilized for glucose concentration detection.[3–9] Among these methods, the electrochemical based biosensors were extensively employed; however, most of the biosensors were enzyme-based.[10–13] The enzyme-modified electrodes suffered from some drawbacks, for instance, complicated immobilization procedures, high cost, instability, and low sensitivity.[14,15] Therefore, it becomes crucial to develop novel electrode nanomaterials that work as electrocatalyst for glucose oxidation and also result in high sensitivity and stability. The performance of nonenzymatic glucose biosensors depends on the morphology of the electrode material. Hence, a variety of nanostructured nanomaterials are utilized to fabricate nonenzymatic biosensors with a high working electrode surface area.

To fabricate nonenzymatic biosensors for glucose detection, significant efforts have been made to synthesize nanomaterials and use them as an electrocatalyst, for example, metals, metal oxides, and their hybrid nanostructures.[16–18] Among different catalysts, nanostructures of copper oxide (CuO) have received considerable interest.[19,20] CuO is the best candidate to fabricate electrochemical based nonenzymatic glucose biosensors, as CuO based biosensors directly oxidizes glucose on the working electrode surface. Moreover, CuO nanostructures possess advanced properties, which are beneficial for designing biosensors.

Research has been concentrated on the shape/dimensions controlling during synthesis of (nano)materials, which have better structural properties that results in enhanced electrochemical performance due to high specific surface area.[21] Previously, a variety of morphologies of CuO nanomaterials have been produced (i.e. nanoparticles, nanowires, nanowhiskers, nanoneedles, nanorods, nanoshuttles, nanoribbons, and nanotubes) using solution-based approach, sonochemical deposition, vapor phase growth, high temperature synthesis, double-jet precipitation, micro-emulsion synthesis, etc.[22] Among these synthesis methods, hydrothermal method presents an environmentally friendly, simple, cost-effective, high-yield, and low-temperature method to synthesize various CuO nanostructures.[23]

Herein, we report hierarchical CuO nanoleaves synthesis in large-quantity by a low-temperature hydrothermal method. As-synthesized CuO nanoleaves were characterized in detail using different techniques. Using engineered CuO nanoleaves, a nonenzymatic electrochemical based biosensor is fabricated. The electrochemical behaviour of the biosensor was investigated for glucose oxidation using cyclic voltammetry (CV) and amperometry techniques. An enhanced electrochemical catalytic behaviour of the fabricated nonenzymatic glucose biosensor was obtained due to CuO nanoleaves high electroactive surface area and superior electro-catalytic activity. The nonenzymatic biosensor displays excellent sensing parameters (i.e., high sensitivity, selectivity, low detection limit, reproducibility, repeatability, and stability. For practical applications, fabricated nonenzymatic glucose biosensors were used to analyze glucose concentration of the real sample (i.e., human serum sample).

Experimental

Reagents.—Copper(II) acetate monohydrate [⩾ 98%, ($Cu(CO_2CH_3)_2{\cdot}H_2O$)], glucose (D-(+) −99.5%), sodium hydroxide (NaOH, 96% purity), cetyltrimethylammonium bromide (CTAB), fructose, sucrose, maltose, lactose, dopamine, uric acid, ascorbic

*Electrochemical Society Member.
[z]E-mail: rahmad5@jmi.ac.in; khosla@yz.yamagata-u.ac.jp

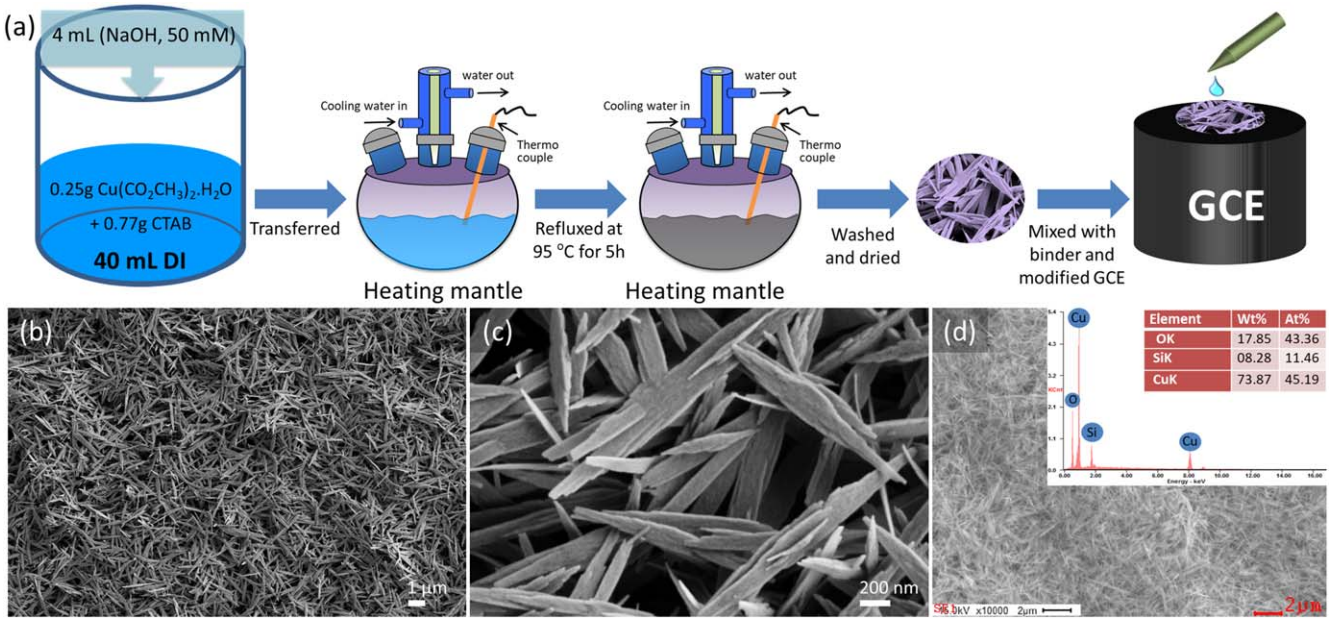

Figure 1. (a) Schematic representation of CuO nanoleaves synthesis, (b)–(d) FESEM images and EDS spectra (inset d) of engineered hierarchical CuO nanoleaves.

acid, butyl carbitol acetate, and Nafion™ solution (20 wt.%) in water and alcohols (lower aliphatic) were acquired from Sigma-Aldrich.

Hierarchical CuO nanoleaves synthesis.—Hierarchical CuO nanoleaves were synthesized using a low-temperature (95 °C) hydrothermal method. For synthesis, 0.25 g $Cu(CO_2CH_3)_2{\cdot}H_2O$ and 0.77 g CTAB were added in 40 ml deionized (DI) water. Next, 4 ml of 50 mM NaOH was added in the above solution while stirring. Then, the above solution was poured into a refluxing pot on a heating mantle and refluxed at 95 °C for 5 h. Finally, black colored precipitates were washed using methanol and DI water to remove impurities and dried at room temperature.

Engineered hierarchical CuO nanoleaves characterization.—The general structural morphologies of engineered hierarchical CuO nanoleaves product was examined by TEM(JEOL-JEM-2010) and FESEM (Hitachi S4700). The crystallinity of hierarchical CuO nanoleaves was studied by XRD. Optical properties and composition of the as-grown hierarchical CuO nanoleaves were characterized by Raman-scattering measurements using excitation source (514.5 nm by Ar^+ laser) and Fourier transform infrared (FTIR) in 400–3000 cm^{-1} range, respectively.

CuO nanoleaves based nonenzymatic glucose biosensor fabrication and measurements.—To fabricate hierarchical CuO nanoleaves based nonenzymatic glucose biosensor; first, the slurry of engineered CuO nanoleaves was prepared after mixing with conducting butyl carbitol acetate binder (8:2 v/v ratio). The prepared slurry (2–6 μl) was cast on cleaned glassy carbon electrode (GCE, 0.071 cm^2) and kept for drying. Finally, Nafion (5 μl) was coated on the electrode (CuO nanoleaves/GCE) surface and kept for overnight at 4 °C.

The cyclic voltammetry (CV) and amperometry (i–t) techniques are utilized for electrochemical measurements. A 3-electrode cell was connected to compact electrochemical analyzer (PalmSens4 potentiostat). Working (Nafion/hierarchical CuO nanoleaves/GCE), counter (Pt), and reference (Ag/AgCl) electrodes are used in the 3-electrode electrochemical cell. The electrochemical experiments are measured in 10 ml 100 mM NaOH solution. Each CV is performed 0 to +0.8 V range (vs Ag/AgCl). During amperometric (i–t) measurement, a fixed potential (+0.6 V) is used. The Nafion/hierarchical CuO nanoleaves/GCE "working electrode" electrodes were kept dry when not in use.

Results and Discussion

Characterizations of engineered hierarchical CuO nanoleaves.—The CuO nanoleaves are synthesized using the hydrothermal method; a schematic representation of synthesis is shown in Fig. 1a. Figures 1b–1d shows the FESEM images and EDS (inset of Fig. 1d) analysis of CuO nanoleaves. The low- and high-magnification images confirm that the CuO nanostructures prepared bear nanoleaves like morphology, and the nanoleaves are uniformly grown in large quantity. EDS analysis of CuO nanoleaves shows that nanoleaves are made of copper (Cu) and oxide (O) elements only (Fig. 1d, inset). EDS spectra shows an additional peak of Si, which is originating from Si substrate used to spread CuO nanoleaves sample for FESEM and EDS analysis.

To get more insightful information, TEM was used to characterize the engineered CuO nanoleaves (Figs. 2a–2c). Low-resolution TEM image of CuO nanoleaves shows the average lengths and widths are about 0.2 μm and 2.1 μm, respectively. Two lattice fringes have 0.27 nm gap, which confirms the monoclinic CuO with [110] lattice fringe (Fig. 2b). Additionally, the SAED pattern validates that the synthesized CuO nanoleaves are single crystalline (Fig. 2c). XRD investigated the crystalline nature of CuO nanoleaves, see spectrum in Fig. 2d. XRD pattern revealed that the synthesized CuO nanoleaves are monoclinic CuO structures and indeed it matched with the JCPDS No. 48–1548, indicating single phase monoclinic CuO. Notably, no other characteristic peaks of impurity or any phases were present.

Figure 3 shows the Raman (a) and FTIR (b) spectra of as-synthesized CuO nanoleaves. The Raman spectra shows the three peaks at 274 cm^{-1}, 325 cm^{-1}, and 603 cm^{-1} that corresponds to the A_g, $B_g^{(1)}$, and $B_g^{(2)}$ modes, respectively (Fig. 3a). These three Raman active modes confirm the single-crystalline nature of CuO nanostructures.[24] Furthermore, the chemical composition and quality of the engineered CuO nanoleaves were investigated by FTIR, shown in Fig. 3b. The strong adsorption characteristic bands at 421 cm^{-1}, 521 cm^{-1}, and 598 cm^{-1} are observed in the spectrum, confirming monoclinic CuO phase formation.[25] Additionally, one weak peak at 1630 cm^{-1} is for the surface hydroxyls and adsorbed water on the surface of CuO nanoleaves.[26]

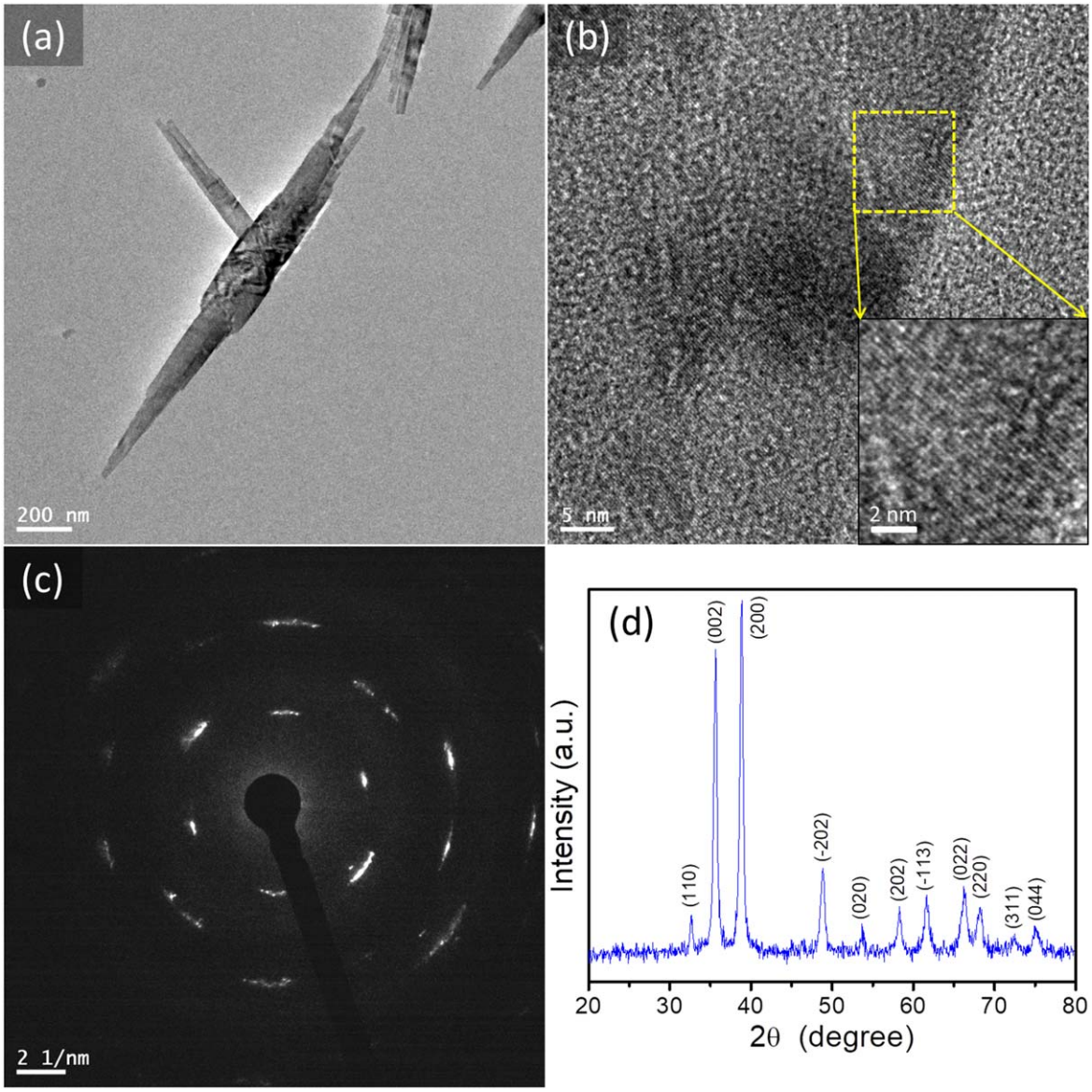

Figure 2. TEM images (a)–(b), SAED pattern (c), and XRD pattern (d) of CuO nanoleaves. Inset b is FFT of selected area.

Electrocatalytic activity analysis.—The electrochemical properties of nonenzymatic biosensor are investigated towards glucose by measuring CV responses in the only buffer (no glucose) and in 100 mM NaOH buffer containing 0.5 mM glucose (Fig. 4). In buffer with no glucose, bare GCE and CuO/GCE non-enzymatic biosensors did not show any peaks (Fig. 4a). Notice that, bare GCE showed no response in buffer containing 0.5 mM glucose (Fig. 4b). From the CV response, it is clear that the CuO nanoleaves modified GCE showed an oxidation peak at 0.6 V due to Cu(II) conversion to Cu (III) in NaOH buffer (Fig. 4b). Marioli and Kuwana proposed the most acceptable glucose detection mechanism in an alkaline medium.[27] They suggested that Cu(III) species act as an electron-transfer medium and glucose gets catalyzed by oxidative Cu(III), which generates gluconolactone that further oxidized to glucose acid. In 0.5 mM glucose, 4 μl CuO nanoleaves modified GCE displayed the highest peak current, which was further utilized to investigate the electrochemical behavior between glucose and CuO nanoleaves/GCE. Figure 4c showed 4 μl CuO nanoleaves/GCE CVs in 100 mM NaOH containing 0.5 mM glucose (scan, 25–200 mV s^{-1}). The calibrated plot shows linear increase in current (correlation coefficient (R^2) = 0.9904) with an increasing scan rate (25–200 mV s^{-1}) (Fig. 4d). The obtained data suggest the surface controlled electrochemical reaction on the surface of CuO nanoleaves/GCE.

To demonstrate the performance of fabricated CuO nanoleaves/GCE nonenzymatic biosensor, current-time (i–t) response of the 4 μl CuO nanoleaves modified GCE was performed using amperometric (gives a better resolution compared to other conventional method) technique in buffer (fixed potential = +0.6 V, vs Ag/AgCl) (Fig. 5). Figure 5a shows the i–t response for CuO nanoleaves modified GCE towards the continuous addition of glucose (0.005–9.89 mM) into the continuously stirred 100 mM NaOH buffer with a rotation speed of 400 rpm. The CuO nanoleaves modified GCE shows a well-defined amperometric i–t response with every addition of glucose concentration with the rapid response time of ~3.5 s. The obtained rapid response clearly indicates fast electron transfer between CuO nanoleaves/GCE and the electrolyte interface while adding different glucose concentrations. From the amperometric i–t response, a plot (i.e., current vs glucose concentration) was plotted, as shown in Fig. 5b. Further, the linear portion of the graph was calibrated, which shows a linear increase of current response from 0.005 to 5.89 mM glucose concentration (inset; Fig. 5b). The linear regression equation [I (μA) = 104.18 (mM) + 17.39] was obtained with high R^2 of

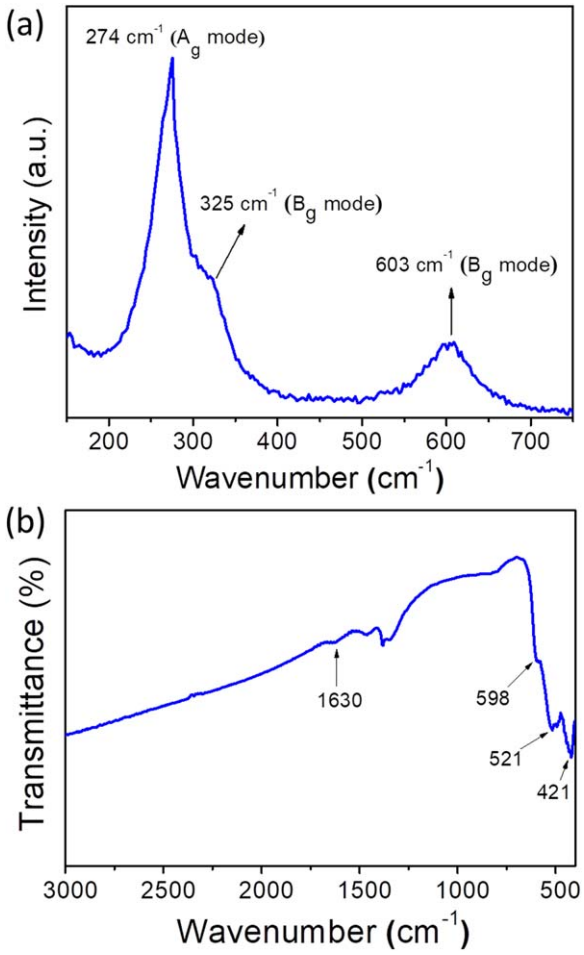

Figure 3. (a) Raman and (b) FTIR spectra of engineered CuO nanoleaves.

Table I. Sensing parameters comparison of the CuO nanostructures based nonenzymatic biosensors.

Modified Electrode	Sensitivity [μA/(mM cm^2)]	Linear range (mM)	Limit of detection (μM)	References
CuO nanosheets-built microtubes/GCE	992.073	0.001–1.164	0.307	28
NiO/CuO/PANI	—	0.02–2.5	0.2	29
CuO NPs and Ag NPs/Fe_3O_4/GCE	—	0.00006–1	0.015	30
NGA—CuO/GCE	223.1	0.01–6.75	2.7	31
CuO—CS/GCE	503	0.05–1	11	32
CuO/S—1@mSiO_2/GCE	5.5	0.005–0.5	0.17	33
AuPd@CuO—MWCNT/GCE	744.98	0.03–9.31	0.11	34
CuO-CoNSs/rGO/3D-KSC/GCE	802.86	0.01–3.95	3.3	35
CuO NPs/GO/GCE	262.52	0.00279–2.03	0.69	36
Ag/CuO NFs/ITO	1347	0.0005–0.5	0.0517	37
CuO NFs/GCE	431	0.006–2.5	0.8	38
CuO nanospheres/GCE	404	Up to 2.6	1	39
CuO NWs/GCE	648.2	—	2	40
NPG—CuO/GCE	374	Up to 12	2.8	41
Au NPs/CuO NWs—MoS_2/Au	872.71	0.0005–5.67	0.5	42
CuO nanodisks/SPCE	627.3	0.002–2.5	0.2	43
CuO polyhedron/GCE	1112	Up to 4	0.22	44
CuO nanoleaves/GCE	1467.32	0.005–5.89	0.012	This work

Abbreviations: NiO, nickel oxide; PANI, polyaniline; NPs, nanoparticles; Fe_3O_4, magnetite, NGA, N-doped graphene aerogel; CS, chitosan; S-1, silicalite-1; mSiO_2, mesoporous silica, Au, gold; Pd, palladium; MWCNT, multi-walled carbon nanotube; CoNSs, Co NSs, cobalt nanostructures; rGO, reduced graphene oxide; KSC, kenaf-stem-derived macroporous carbon; ITO, indium tin oxide; GO, graphene oxide; NFs, nanofibers; NWs, nanowires; NPG, nanoporous gold; MoS_2, molybdenum disulfide; SPCE, screen printed carbon electrodes.

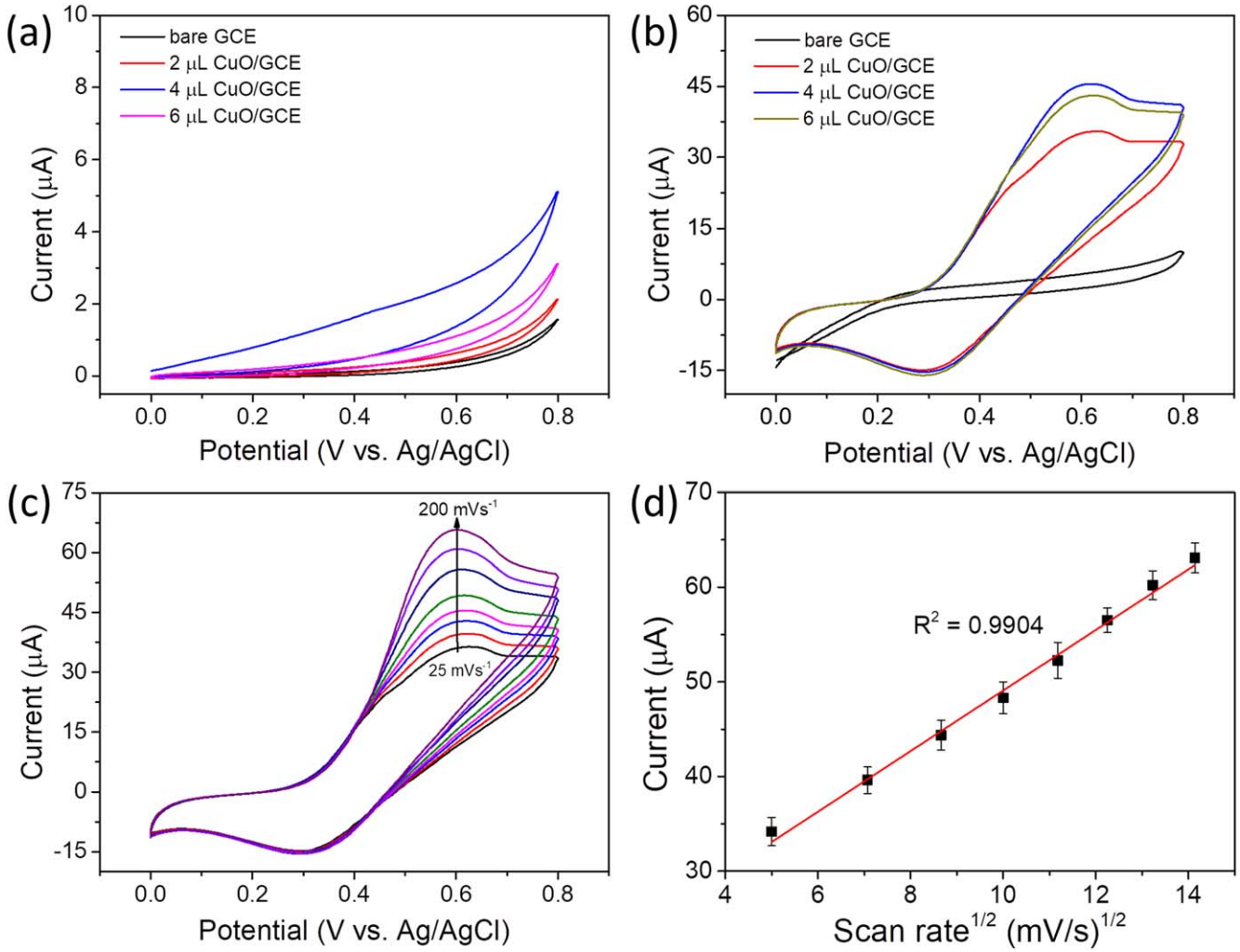

Figure 4. Cyclic voltammograms (CVs) of the bare GCE and 2–6 μl CuO nanoleaves modified GCE (CuO nanoleaves/GCE) in the buffer (no glucose) (a) and in 0.5 mM glucose (b) in 100 mM NaOH measured with 50 mV s^{-1} scan rate, CVs of 4 μl CuO nanoleaves/GCE in 100 mM NaOH containing 0.5 mM glucose from 25 to 200 mV s^{-1} scan rates, (c), and calibrated plot showing square root of scan rate vs CV peak current (d).

Table II. Analysis of glucose concentration in human serum.

Serum sample	Added glucose (mM)	Found glucose (mM)	Recovery (%)	RSD (%), (n = 3)
Human blood serum	—	4.95	—	1.8
	0.5	5.42	99.4	3.2
	1	5.98	100.5	2.9
	2	7.14	102.7	2.5
	4	9.24	103.2	2.7

0.9955 (inset, Fig. 5b). The sensitivity of the CuO nanoleaves/GCE nonenzymatic biosensor was estimated to be 1467.32 μA/(mM cm^2) by dividing the slope (104.18 μA/mM) of calibration curve with geometrical surface of GCE (0.071 cm^2). The detection limit is 12 nM (S/N = 3). Obtained analytical performance such as linear range, sensitivity, and detection limit has been compared with previous literatures in Table I. From the compared literatures in Table I, the linear range and sensitivity were better than most nonenzymatic biosensors. However, the limit of detection is superior. Better analytical parameters are due to the excellent electrocatalytic nature of CuO nanoleaves modified GCE nonenzymatic biosensor.

Anti-interference, stability, repeatability, and reproducibility analysis.—Selectivity test of the fabricated CuO nanoleaves/GCE nonenzymatic biosensor was studied by introducing possible interference species in the 100 mM NaOH buffer during amperometric measurement. Figure 5c shows the i–t response of selectivity measurement with the glucose addition (1 mM) followed by 0.1 mM possible interfering species (i.e. fructose, maltose, sucrose, lactose, dopamine, uric acid, and ascorbic acid) addition and the final 1 mM glucose addition. The biosensor responded rapidly after addition of glucose; however, there is no noticeable peak current with addition of interfering species; see histogram in Fig. 5d. Additionally, almost same i–t response was noticed for 1 mM glucose addition in the presence of all these interfering species, suggests good selectivity nature of the biosensor. Hence, the fabricated nonenzymatic biosensor can serve as a selective electrochemical based nonenzymatic biosensor for glucose detection even in complex medium (i.e., human serum).

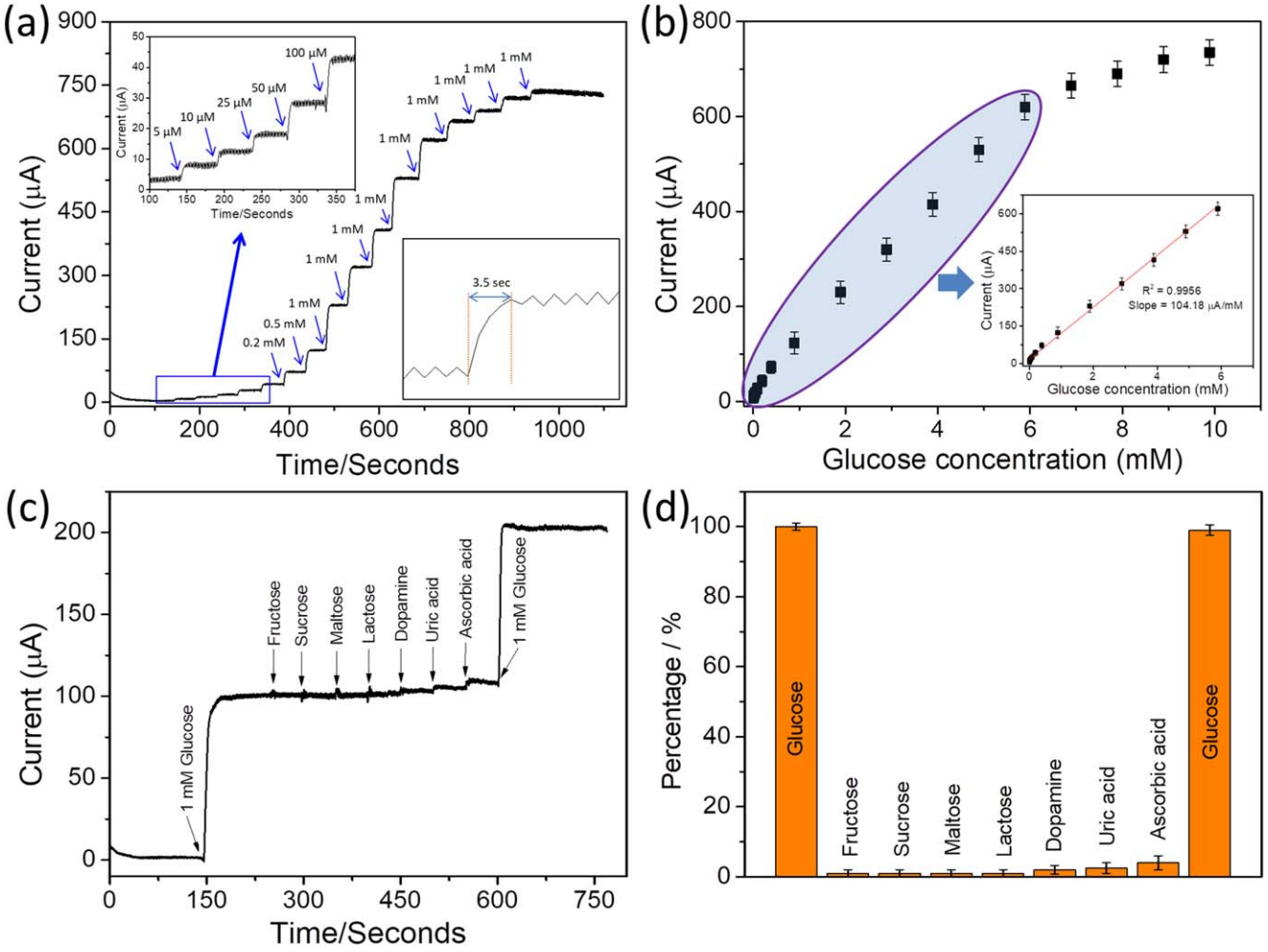

Figure 5. Amperometric response of 4 μl CuO nanoleaves/GCE with step-wise glucose addition in 100 mM NaOH at a fixed potential (+0.6 V vs Ag/AgCl) (upper inset is magnified view of response toward low glucose concentration addition and lower inset is showing the response time of the sensor) (a), amperometric current response vs glucose concentration showing linear and non-linear regions (inset: calibrated current-glucose concentration curve of linear region) (b), amperometric response showing anti-interference measurement of CuO nanoleaves/GCE with glucose (1 mM), 0.1 mM each possible interfering species (i.e. fructose, sucrose, maltose, lactose, uric acid, dopamine, and ascorbic acid), and finally 1 mM glucose addition (c), and histogram showing CuO nanoleaves/GCE response for addition of glucose and interfering species (d).

Next, the long-term storage stability of the CuO nanoleaves modified GCE nonenzymatic biosensor was tested and stored at room temperature. CV responses of the biosensors were measured for periods of 3 d. After 21 d, the biosensor showed only 3.25% decrease to its initial current response (Fig. 6a, shows cv of day 1 and 21 d), which revealed that the CuO nanoleaves modified GCE is stable and suitable for practical glucose detection. To evaluate the reproducibility, 5 CuO nanoleaves modified GCE electrodes were fabricated in similar conditions, and their CV responses were measured. All the biosensors showed almost the same response with 2.6% relative standard deviation (RSD) (Fig. 6b), confirming the biosensor's acceptable fabrication reproducibility. Furthermore, the repeatability CuO nanoleaves modified GCE biosensor was tested by 10 consecutive CV analysis in 0.5 mM glucose, which showed current response with RSD of 3.4%, confirming the satisfactory repeatability of the biosensor.

Application of the CuO nanoleaves/GCE biosensor in real serum sample.—To test the practical application of CuO nanoleaves modified GCE nonenzymatic biosensor, a serum sample from the healthy human was obtained and tested using our biosensor. During measurement, the amount of buffer in the electrochemical cell was kept at 9.5 ml and 0.5 ml real (serum, or serum and spiked known glucose concentration) samples were added in the buffer. In the serum sample, the glucose concentration was found to be 4.95 ± 0.05, which was similar to the glucose concentration measured in the hospital using commercially available glucose biosensor. Further, known glucose concentration samples were added in the serum sample and their recoveries were estimated, shown in Table II. Recoveries of the spiked glucose concentration were in the acceptable range, confirming the possibility of using our nonenzymatic glucose biosensor in real samples.

Conclusions

In summary, using a low-temperature hydrothermal synthetic method, we engineered CuO nanoleaves like nanostructures in large quantity and successfully utilized to construct sensitive electrochemical based nonenzymatic glucose biosensor. In 3-electrode system, the electrochemical performance of the designed CuO nanoleaves modified GCE biosensor was investigated towards glucose. The biosensor demonstrated excellent electrocatalytic properties, which resulted in good sensitivity (1467.32 μA/(mM cm^2)), linear range up to 5.89 mM, response time (3.5 s), and detection limit (12 nM). Moreover, the biosensor demonstrates good selectivity, reproducibility, stability, and repeatability. Additionally, the biosensor was evaluated for real sample analysis with good recovery. Therefore, we believe our engineered CuO nanoleaves based nonenzymatic biosensor can pave the way to detect glucose in low glucose level samples (i.e., saliva, tear, sweat).

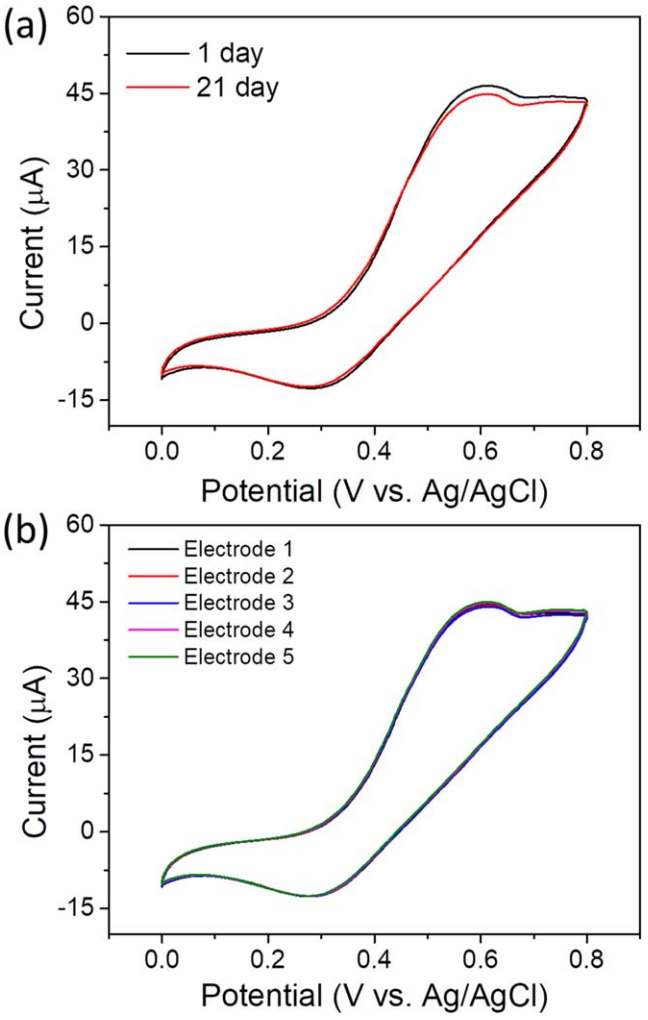

Figure 6. (a) Comparative CV responses of CuO nanoleaves modified GCE biosensor in 0.5 mM glucose on day 1 and after 21 d storage and (b) reproducibility test of the biosensor.

Acknowledgments

Funding from the Department of Biotechnology (DBT), Government of India, supported the research reported in this publication. This work was supported in part by JSPS KAKENHI Grant Number JP17H01224, JP18H05471, JP19H01122, JST COI Grant Number JPMJCE1314, JST -OPERA Program Grant Number JPMJOP1844, JST -OPERA Program Grant Number JPMJOP1614, and the Cabinet Office (CAO), Cross-ministerial Strategic Innovation Promotion Program (SIP), "An intelligent knowledge processing infrastructure, integrating physical and virtual domains" (funding agency: NEDO). Authors are thankful to the Department of Biotechnology, Government of India for the Ramalingaswami Fellowship Award to R.A.

ORCID

Rafiq Ahmad https://orcid.org/0000-0001-6345-3507
Ajit Khosla https://orcid.org/0000-0002-2803-8532

References

1. Y. Marunaka, "Roles of interstitial fluid pH in diabetes mellitus: Glycolysis and mitochondrial function." *World Journal of Diabetes*, **6**, 125 (2015).
2. C. P. Domingueti, L. M. S. A. Dusse, M. das Graças Carvalho, L. P. de Sousa, K. B. Gomes, and A. P. Fernandes, "Diabetes mellitus: The linkage between oxidative stress, inflammation, hypercoagulability and vascular complications." *J. Diabetes Complicat.*, **30**, 738 (2016).
3. M. A. Akhtar, R. Batool, A. Hayat, D. Han, S. Riaz, S. U. Khan, M. Nasir, M. H. Nawaz, and L. Niu, "Functionalized graphene oxide bridging between enzyme and Au-sputtered screen-printed interface for glucose detection." *ACS Appl. Nano Mater.*, **2**, 1589 (2019).
4. R. Ahmad, M. Vaseem, N. Tripathy, and Y.-B. Hahn, "Wide linear-range detecting nonenzymatic glucose biosensor based on CuO nanoparticles inkjet-printed on electrodes." *Anal. Chem,.*, **85**, 10448 (2013).
5. V. E. Coyle, A. E. Kandjani, M. R. Field, P. Hartley, M. Chen, Y. M. Sabri, and S. K. Bhargava, "Co3O4 needles on Au honeycomb as a non-invasive electrochemical biosensor for glucose in saliva." *Biosens. Bioelectron.*, **141**, 111479 (2019).
6. J. Xiao, Y. Liu, L. Su, D. Zhao, L. Zhao, and X. Zhang, "Microfluidic chip-based wearable colorimetric sensor for simple and facile detection of sweat glucose." *Anal. Chem.*, **91**, 14803 (2019).
7. R. Ahmad, M. Khan, M. R. Khan, N. Tripathy, M. I. R. Khan, P. Mishra, M. A. Syed, and A. Khosla, "Nano-donuts shaped nickel oxide nanostructures for sensitive non-enzymatic electrochemical detection of glucose." *Microsyst. Technol.*, 1 (2020).
8. W. Han, H. He, L. Zhang, C. Dong, H. Zeng, Y. Dai, L. Xing, Y. Zhang, and X. Xue, "A self-powered wearable noninvasive electronic-skin for perspiration analysis based on piezo-biosensing unit matrix of enzyme/ZnO nanoarrays." *ACS Appl. Mater. Interfaces*, **9**, 29526 (2017).
9. R. Ahmad, M. Khan, N. Tripathy, M. I. R. Khan, and A. Khosla, "Hydrothermally synthesized nickel oxide nanosheets for nonenzymatic electrochemical glucose detection." *J. Electrochem. Soci.*, **167**, 107504 (2020).
10. R. Ahmad, T. Mahmoudi, M.-S. Ahn, and Y.-B. Hahn, "Recent advances in nanowires-based field-effect transistors for biological sensor applications." *Biosens. Bioelectron.*, **100**, 312 (2018).
11. T. Liang et al., "Rising mesopores to realize direct electrochemistry of glucose oxidase toward highly sensitive detection of glucose." *Adv. Funct.*, **44**, 1903026 (2019).
12. R. Ahmad, N. Tripathy, J.-H. Park, and Y.-B. Hahn, "A comprehensive biosensor integrated with a ZnO nanorod FET array for selective detection of glucose, cholesterol and urea." *Chem. Commun.*, **51**, 11968 (2015).
13. J. Yoon, S. N. Lee, M. K. Shin, H.-W. Kim, H. K. Choi, T. Lee, and J.-W. Choi, "Flexible electrochemical glucose biosensor based on GOx/gold/MoS2/gold nanofilm on the polymer electrode." *Biosens. Bioelectron.*, **140**, 111343 (2019).
14. K. Puttananjegowda, A. Taksi, and S. Thomas, "Perspective-electrospun nanofibrous structures for electrochemical enzymatic glucose biosensing: A perspective." *J. Electrochem. Soci.*, **167**, 037553 (2020).
15. M. A. Deshmukh, B.-C. Kang, and T.-J. Ha, "Non-enzymatic electrochemical glucose sensors based on polyaniline/reduced-graphene-oxide nanocomposites functionalized with silver nanoparticles." *J. Mater. Chem. C*, **8**, 5112 (2020).
16. E. Sehit and Z. Altintas, "Significance of nanomaterials in electrochemical glucose sensors: An updated review (2016-2020)." *Biosens. Bioelectron.*, **159**, 112165 (2020).
17. T. N. H. Nguyen, X. Jin, J. K. Nolan, J. Xu, K. V. H. Le, S. Lam, Y. Wang, M. A. Alam, and H. Lee, "Printable nonenzymatic glucose biosensors using carbon nanotube-PtNP nanocomposites modified with AuRu for improved selectivity." *ACS Biomater. Sci. Eng.*, **6**, 5315 (2020).
18. M. Adeel, M. M. Rahman, I. Caligiuri, V. Canzonieri, F. Rizzolio, and S. Daniele, "Recent advances of electrochemical and optical enzyme-free glucose sensors operating at physiological conditions." *Biosens. Bioelectron.*, **165**, 112331 (2020).
19. M. Bidikoudi and E. Kymakis, "Novel approaches and scalability prospects of copper based hole transporting materials for planar perovskite solar cells." *J. Mater. Chem. C*, **7**, 13680 (2019).
20. U. T. Khatoon, K. M. Mantravadi, and G. V. S. N. Rao, "Strategies to synthesise copper oxide nanoparticles and their bio applications-A review." *Mater. Sci. Techno.*, **34**, 2214 (2018).
21. H. Ehtesabi, "Carbon nanomaterials for salivary-based biosensors: A review." *Mater. Today Chem.*, **17**, 100342 (2020).
22. A. S. Zoolfakar, R. A. Rani, A. J. Morfa, A. P. O'Mullane, and K. Kalantar-zadeh, "Nanostructured copper oxide semiconductors: A perspective on materials, synthesis methods and applications." *J. Mater. Chem. C*, **2**, 5247 (2014).
23. H. Lee, X. Wu, and L. Sun, "Copper-based homogeneous and heterogeneous catalysts for electrochemical water oxidation." *Nanoscale*, **12**, 4187 (2020).
24. J. Fang and Y. Xuan, "Investigation of optical absorption and photothermal conversion characteristics of binary CuO/ZnO nanofluids." *RSC Adv.*, **7**, 56023 (2017).
25. M. Elango, M. Deepa, R. Subramanian, and A. M. Musthafa, "Synthesis, characterization, and antibacterial activity of polyindole/Ag-Cuo nanocomposites by reflux condensation method." *Polymer-Plastics Techno. Eng.*, **57**, 1440 (2018).
26. A. S. Ethiraj and D. J. Kang, "Synthesis and characterization of CuO nanowires by a simple wet chemical method." *Nanoscale Res. Lett.*, **7**, 70 (2012).
27. M. Marioli and T. Kuwana, "Electrochemical characterization of carbohydrate oxidation at copper electrodes." *Electrochim. Acta*, **37**, 1187 (1992).
28. P. Yang, X. Wang, C. Ge, X. Fu, X. Y. Liu, H. Chai, X. Guo, H. C. Yao, Y. X. Zhang, and K. Chen, "Fabrication of CuO nanosheets-built microtubes via Kirkendall effect for non-enzymatic glucose sensor." *Appl. Surf. Sci.*, **494**, 484 (2019).
29. K. Ghanbari and Z. Babaei, "Fabrication and characterization of non-enzymatic glucose sensor based on ternary NiO/CuO/polyaniline nanocomposite." *Anal. Biochem.*, **498**, 37 (2016).
30. M. Baghayeri, M. Nodehi, A. Amiri, N. Amirzadeh, R. Behazin, and M. Z. Iqbal, "Electrode designed with a nanocomposite film of CuO Honeycombs/Ag nanoparticles electrogenerated on a magnetic platform as an amperometric glucose sensor." *Anal. Chim. Acta*, **1111**, 49 (2020).

31. J. Yang, W. Tan, C. Chen, Y. Tao, Y. Qin, and Y. Kong, "Nonenzymatic glucose sensing by CuO nanoparticles decorated nitrogen-doped graphene aerogel." *Mater. Sci. Eng. C*, **78**, 210 (2017).
32. M. Figiela, M. Wysokowski, M. Galinski, T. Jesionowski, and I. Stepniak, "Synthesis and characterization of novel copper oxide-chitosan nanocomposites for non-enzymatic glucose sensing." *Sens. Actuators B: Chem.*, **272**, 296 (2018).
33. X. Cheng, H. Zhao, W. Huang, J. Chen, S. Wang, J. Dong, and Y. Deng, "Rational design of yolk–shell CuO/silicalite-1@mSiO2 Composites for a high-performance nonenzymatic glucose biosensor." *Langmuir*, **34**, 7663 (2018).
34. Y. Tang, Q. Liu, Z. Jiang, X. Yang, M. Wei, and M. Zhang, "Nonenzymatic glucose sensor based on icosahedron AuPd@CuO core–shell nanoparticles and MWCNT." *Sens. Actuators B: Chem.*, **251**, 1096 (2017).
35. L. Wang, L. Xu, Y. Zhang, H. Yang, L. Miao, C. Peng, and Y. Song, "Copper oxide-cobalt nanostructures/reduced graphene oxide/biomass-derived macroporous carbon for glucose sensing." *ChemElectroChem*, **5**, 501 (2018).
36. J. Song, L. Xu, C. Zhou, R. Xing, Q. Dai, D. Liu, and H. Song, "Synthesis of graphene oxide based CuO nanoparticles composite electrode for highly enhanced nonenzymatic glucose detection." *ACS Appl. Mater. Interfaces*, **5**, 12928 (2013).
37. B. Zheng, G. Liu, A. Yao, Y. Xiao, J. Du, Y. Guo, D. Xiao, Q. Hu, and M. M. F. Choi, "A sensitive AgNPs/CuO nanofibers non-enzymatic glucose sensor based on electrospinning technology." *Sens. Actuators B*, **195**, 431 (2014).
38. X. L. Zhu, X. Gan, J. Wang, T. Chen, and G. X. Li, "A new reduction route of hypoxanthine and its nonenzymatic detection based on silver nanoparticles." *J. Mol. Catal. A: Chem.*, **239**, 201 (2005).
39. E. Reitz, W. Jia, M. Gentile, Y. Wang, and Y. Lei, "CuO nanospheres based nonenzymatic glucose sensor." *Electroanalysis*, **20**, 2482 (2008).
40. Y. Zhang, Y. Liu, L. Su, Z. Zhang, D. Huo, C. Hou, and Y. Lei, "CuO nanowires based sensitive and selective non-enzymatic glucose detection." *Sens. Actuators B*, **191**, 86 (2014).
41. X. Xiao, M. Wang, H. Li, Y. Pan, and P. Si, "Non-enzymatic glucose sensors based on controllable nanoporous gold/copper oxide nanohybrids." *Talanta*, **125**, 366 (2014).
42. J. Bao, Y. Qi, D. Huo, J. Hou, X. Geng, M. Samalo, Z. Liu, H. Luo, M. Yang, and C. Hou, "A sensitive and selective non-enzymatic glucose sensor based on AuNPs/CuO NWs-MoS2 modified electrode." *J. Electrochem. Soci.*, **166**, B1179 (2019).
43. M. S. Jagadeesan, K. Movlaee, T. Krishnakumar, S. G. Leonardi, and G. Neric, "One-step microwave-assisted synthesis and characterization of novel CuO nanodisks for non-enzymatic glucose sensing." *J. Electroanal. Chem.*, **835**, 161 (2019).
44. C. Kong, L. Tang, X. Zhang, S. Sun, S. Yang, X. Song, and Z. Yang, "Templating synthesis of hollow CuO polyhedron and its application for nonenzymatic glucose detection." *J. Mater. Chem. A*, **2**, 7306 (2014).